INTERPRETATION OF AC IMPEDANCE MEASUREMENTS IN SOLIDS*

J. Ross Macdonald

Department of Physics and Astronomy
University of North Carolina
Chapel Hill, North Carolina 27514

INTRODUCTION

In order to use solid materials most effectively in solid electrolyte applications, they need to be characterized as fully as is practical. Here, one useful method of electrical response characterization will be discussed: measurement of the response when a small-signal sinusoidal potential difference is applied across a sample. A great deal more can be learned from the frequency and temperature dependence of the resulting impedance than from ordinary DC or single-frequency AC conductance measurements alone.

An exact solution of an idealized model of a system involving homogeneous material between two identical plane parallel electrodes separated by a distance ℓ has recently been given.[1,2] It incorporates the following five physical processes: charge separation, adsorption-desorption and charge transfer at electrodes, diffusion effects, and bulk generation-recombination (G/R). Many impedance results[3,4] and considerable background information[2] have already been presented; space limitation precludes their recapitulation here. Instead, the present work will concentrate on the use of earlier and current complex impedance plane results to illustrate methods of characterizing materials in terms of (a) pertinent equivalent circuits and (b) basic quantities such as mobilities, reaction rates, etc. derivable from equivalent circuit elements.

PERTINENT PARAMETERS

Figure 1 shows the equivalent circuit following most directly from the model.[1] All circuit elements will be given for unit electrode area. In general, $C_i(0) \equiv C_{i0}$ is finite and $R_i(\infty)$ is zero. Thus, the circuit necessarily incorporates an $\omega = 0$ resistive path, R_D, and as $\omega \to \infty$, ordinary bulk response involving the geometric capacitance $C_g \equiv \varepsilon/4\pi\ell$, and the bulk resistance, $R_\infty \equiv \ell/[(ez_e)(\mu_n n_e + \mu_p p_e)]$. Here $R_\infty^{-1} \equiv R_E^{-1} + R_D^{-1}$; ε is the dielectric constant of the material; μ_n and μ_p are the mobilities of negative and positive charges of equilibrium concentrations n_e and p_e; and the valence numbers, z_n and z_p of these charges have, for simplicity, been taken equal to z_e here. For an intrinsic conduction situation, $n_e \equiv p_e \equiv c_i$. The dielectric relaxation time $\tau_D \equiv R_\infty C_g$ is also equal to $\varepsilon/4\pi\sigma$, where $\sigma \equiv \ell/R_\infty$ is the high-frequency limiting conductivity of the material. It is often convenient to use the normalized frequency $\Omega \equiv \omega\tau_D$ and to normalize circuit elements with R_∞ and C_g. Such normalization will be denoted by a subscript "N." Thus, $R_{DN} \equiv R_D/R_\infty$, $C_{iN} \equiv C_i/C_g$, etc. Also, let $\pi_m \equiv \mu_n/\mu_p$.
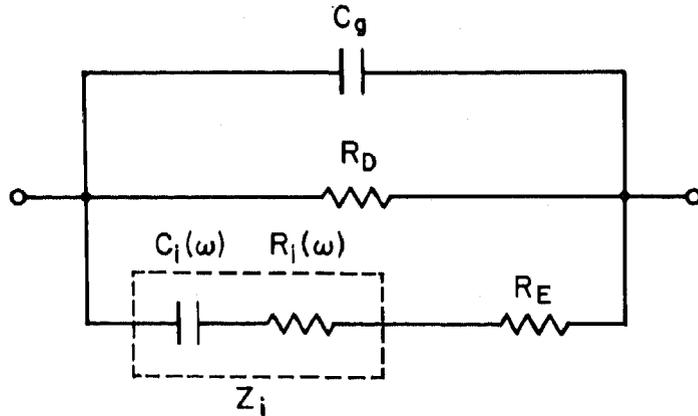

Fig. 1   General equivalent circuit following from theory.

For simplicity, the present analysis will deal primarily with complete blocking at the electrodes of mobile positive charges. Negative charges, however, may react at the electrodes with a heterogeneous rate constant k_n, related to a dimensionless boundary parameter r_n by $k_n \equiv (D_n/\ell)r_n = (kT\mu_n/\ell ez_e)r_n$. Here k is Boltzmann's constant, T the absolute temperature, and ℓ the proton charge. When $r_n = 0$, negative charges are also completely blocked, a $(r_p, r_n) = (0,0)$ situation. In the presence of adsorption, r_n becomes complex,[5,6] and one must introduce both its low-frequency limiting value r_{n0} and its high-frequency value $r_{n\infty}$ as well as the internal adsorption relaxation time τ_{An}. Generation/recombination effects[7,8] will be largely neglected in the present work. Define N_e as the net concentration of extrinsic centers, assumed fully dissociated, and N_i as the concentration of neutral intrinsic centers before any dissociation. Then $\chi \equiv N_e/2z_e c_i$ will determine the degree of extrinsic conduction and c_i/N_i the amount of intrinsic dissociation present.

EQUIVALENT CIRCUITS

Although the model[1] yields relatively simple expressions for the R_{EN} and R_{DN} of Fig. 1, that for $Z_{iN} \equiv R_{iN} + (i\Omega C_{iN})^{-1}$ is very complicated, making it often difficult to use. Further, many of the effects of the five principal processes incorporated in the model are buried in the frequency dependence of $C_i(\omega)$ and $R_i(\omega)$. Therefore, it is worthwhile to consider other kinds of circuits which may still represent the physical processes present adequately.

All linear circuits not containing inductance can be represented by either the Maxwell model, the left circuit of Fig. 2, or the Voigt model, the right circuit. By proper choice of element values, these two circuits can be made to have the same total impedance Z_T at all frequencies. The right-hand circuit of Fig. 2 has been used to represent N-layer Maxwell-Wagner (M-W) interfacial polarization.[9,10] In this theory, it is assumed that the material involves N separate layers, each with its specific dielectric constant and conductivity. The two-layer model, being simplest, has often been used. It could be appropriate for a two-phase material such as a pressed and/or sintered compact in which somewhat conducting particles were dispersed in a matrix of
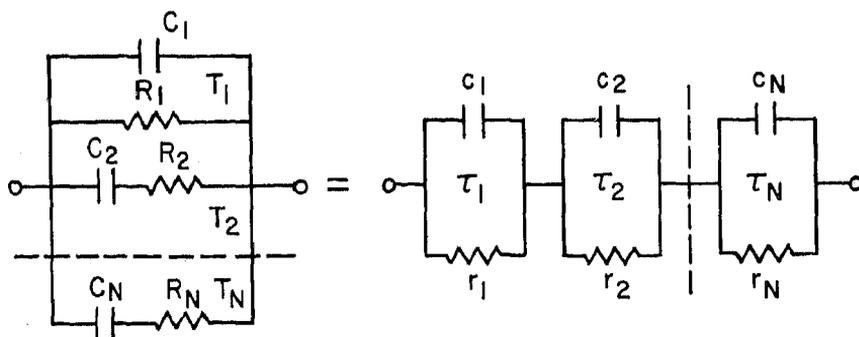
Fig. 2   Two equivalent circuits which may have the same
         overall impedance.

different conductivity or, in the absence of a matrix, the
particles themselves might have a more or less homogeneous
central region surrounded by oxygen-rich surface layers.
Alternatively, the two layers might represent bulk and sur-
face regions of a macroscopic sample. The two-layer model
has been modified in various ways: for example by consider-
ing it as a two-layer capacitor with a continuous distribu-
tion of relaxation times[11] or by assuming[12] Schottky bar-
riers are present in one of the layers and may cause the re-
sistance and capacitance of the layer to depend upon the po-
tential difference across it.

Notice that the M-W model even with the above generali-
zation is rather simplistic. In a real N-layer M-W material,
one might expect that each layer or phase could separately
involve many of the physical effects discussed above.

Since the present homogeneous-material model can often
lead to $Z_T(\omega)$ response of essentially just the kind predicted
by the inhomogeneous-material M-W model with N = 2 or 3, un-
less it is known that the material is strongly inhomogeneous,
it seems wise first to try to analyze its response on the
basis of a homogeneous model. If this is insufficient, then
two such homogeneous models connected in series and involving
different parameters might be considered. While it may some-
times be easy to mistake the response of a homogeneous sys-
tem for an inhomogeneous one, distinction between them can
frequently be made on the basis of their possibly different
responses to a change of electrode separation distance, ℓ.

Although the two circuits of Fig. 2 may be made en-
tirely equivalent electrically, they may not be equivalent
in terms of interpretive power for characterization pur-
poses. When these circuits are thought to be appropriate,
which one should be used? If each of the main processes
which lead to the electrical response considered separately
produces one of the series RC branches of the left-hand cir-
cuit, then this circuit will generally be more appropriate
than the right-hand one, which will then characteristically
involve mixtures of processes for each parallel RC section.
From this point of view, dielectric relaxation with a dis-
tribution of relaxation times (N finite or infinite) seems
better represented, as is customary, by the left than the
right circuit. For a M-W system, involving layers physi-
cally in series, however, clearly the right hand one should
be employed.

Further, when impedances or admittances (or complex di-
electric constants[13]) are to be plotted as parametric func-
tions of frequency in the complex plane, admittance plane
(or complex dielectric constant) plots will be more appro-
priate when the left-hand circuit is the preferred one and
impedance plane plots will be more appropriate for the right
one.[2] For the present homogeneous model where, at least in
the limit of very loosely coupled processes, each parallel
RC section is associated with a separate process or physi-
cal region, impedance plane plotting is therefore preferred
and will result in a connected series of arcs, each again
associated with a single process and a single RC section.
Analysis will then be greatly simplified since mixture of
processes and effects will be avoided.

While straightforward transformation equations exist
which lead from known values of the elements of the right-
hand circuit of Fig. 2 to values of the left-hand circuit
elements, direct solutions for the reverse transformation
are not very practical for N > 2. It would therefore be
desirable if the present model led directly to a Voigt type
of circuit instead of that of Fig. 1. Although it is not
self-evident that the model can often be well represented by
a Voigt circuit, it indeed can be.[3,4]

The resulting approximate circuit is shown in Fig. 3-a.
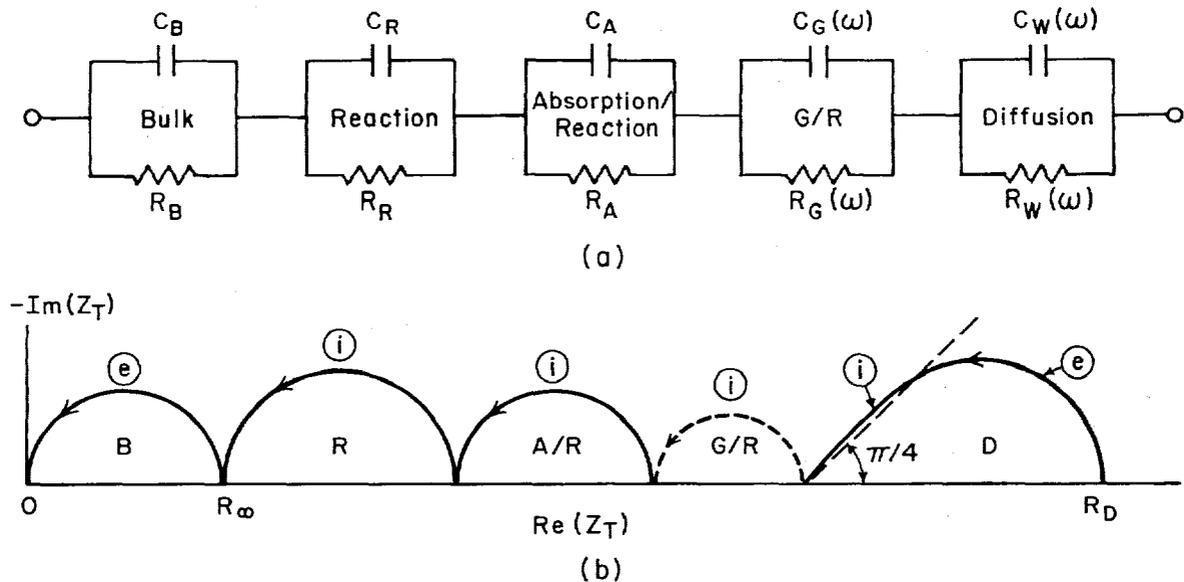This is an N = 5 Voigt system except that the last two

Fig. 3 (a) Equivalent circuit following from the present model. (b) Possible $Z_T^*(\omega)$ complex plane plot consistent with the circuit in (a).

sections may involve frequency dependent elements. The des-
ignations of the sections are appropriate only for very
loose coupling; i.e., each time constant must differ from
all others by at least a factor of 10^2. Surprisingly, how-
ever, it turns out, based on least squares analysis of ex-
act model results, that the circuit shown here is often an
excellent approximation even in the close-coupled case.
Then we must designate the elements as C_k and R_k, with k =
1,2,...,5. It is hoped that future work will reveal how
these parameters, each of which may in the close-coupled
case depend on all processes, can be related to the basic
material characterization parameters.

For simplicity, most of the following results will ap-
ply only to the intrinsic-conduction loosely coupled case.
Unless the recombination internal relaxation time is much
greater than τ_D, contrary to the intrinsic-conduction pre-
diction of the Langevin diffusion theory of the bimolecular
recombination constant,[2] it turns out that the G/R contribu-
tion, Z_G, to $Z_T \stackrel{\sim}{=} \sum_{k=1}^{5} Z_k$, is negligible compared to the other
contributions to Z_T. When it is not negligible, C_G and R_G
may or may not be frequency independent,[2] depending on the
value of τ_m. Possible generation/recombination effects will
be considered in detail elsewhere.

Fig. 3-b is a plot of $Z_T^* \equiv \text{Re}(Z_T) - i[\text{Im}(Z_T)]$ in the
complex plane for a loosely coupled situation. Arrows in-
dicate the direction of increasing frequency. Frequently,
not all these arcs will be significant at the same time.
The G/R arc is shown dotted since it may be negligible un-
der most conditions and may be either semicircular or simi-
lar in shape to the finite-length Warburg diffusion arc[3]
shown at the right. The sizes of the arcs depend on the
process parameters; they may thus vary widely in relative
magnitude. They have only been shown roughly similar here
in order to fit all five on the same diagram. Further, the
order in which specific arcs appear may vary greatly depend-
ing on the time constants involved. The theory does not
allow the A/R arc to occur at higher frequencies than the R
arc, however. Further, in cases of practical interest, the
B arc will always lie at the left.

The present model, when well approximated by the circuit

of Fig. 3-a, leads to

$$Z_{TN} \equiv \sum_{k=1}^{5} Z_{kN} \cong \sum_{k=1}^{5} \left\{ \frac{(1 - \delta_{k5})R_{kN}}{(1 + i\Omega\tau_{kN})} + \left(\frac{\delta_{k5}}{\pi_m}\right)\left(\frac{\tanh(i\Omega\tau_{kN})^{1/2}}{(i\Omega\tau_{kN})^{1/2}}\right) \right\},$$

(1)

where δ_{kj} is Kronecker's delta and $\tau_{kN} \equiv R_{kN}C_{kN}$. In the usual case where the normalized bulk time constant is well separated from the others $(\tau_{kN} \gg \tau_{1N} \cong \tau_{BN} \cong 1$, $k = 2$ to 5), $R_{1N} \cong R_{BN} \cong 1$ and $C_{1N} \cong C_{BN} \cong 1$. Approximate expressions for the other normalized parameters will be discussed in the next section. Note that each semicircle of Fig. 3-b is associated with one of the $k = 1$ to 4 terms, while the $k = 5$ term accounts approximately for finite-length Warburg response.

Sometimes, experimental arcs are depressed[4] (less than a semicircle), possibly arising from a continuous distribution in one or more of the elements of the given process. Under some circumstances, the present model can yield some depression for the reaction arc without distributed elements, however.[4] Depression can be accounted for heuristically in the present approximate approach by writing[4,14] each $k = 1$ to 4 denominator in (1) in the Cole-Cole[13] form $[1 + (i\Omega\tau_{kN})^{1-\alpha_k}]$, where α_k is a distribution parameter which is zero when there is no distribution.[13] It is sometimes found experimentally that the straight line portion of the diffusion arc lies at an angle different from the theoretical Warburg value of $\pi/4$. One possible way of accounting heuristically for such a result is to raise the $k = 5$ $[\tanh( )^{1/2}]/( )^{1/2}$ quotient to the $(1 - \alpha_5)$ power, with $-1 \leq \alpha_5 < 1$. This modification is quite similar in effect to the skewed-arc Davidson-Cole heuristic relaxation distribution modification.[15] It is likely to be more appropriate here, however, since the approximate $k = 5$ term in Eq. (1) follows directly from the detailed model when $\alpha_5 = 0$.

Finally, the circled "e's" and "i's" in Fig. 3-b stand for extensive and intensive. Here "intensive" means that the R and C parameters of the arc are independent of ℓ. Arcs or portions of arcs which are extensive will, in contrast, change with change in ℓ, helping somewhat to identify

an experimental arc as being associated with a specific
process in the loosely coupled case.

CHARACTERIZATION RESULTS AND POSSIBILITIES

There are many different ways to plot frequency re-
sponse results. Some of them have been discussed else-
where.[2] It has been found that the present model (with
$\alpha_k = 0$ for all k) can lead to frequency dependence of C_p,
the overall parallel capacitance of the system, of the form
ω^{-m} over an appreciable range with m = 0.5, 1, 1.5, and 2
and even some intermediate values. For characterization,
however, only a complex-plane $Z_T^*(\omega)$ plot is needed. Then,
the data may be analyzed with as many terms of Eq. (1) as
required, preferably by nonlinear least squares fitting (of,
e.g., $Im[Z_T(\omega)]$), to determine the pertinent R and C param-
eters. Equation (1) may be transformed to unnormalized
form by omitting N's, multiplying the last term by R_∞, and
changing Ω to ω. Once $R_1 \cong R_\infty$ and $C_1 \cong C_g$ values have been
found, the remaining parameter estimates may be normalized
with them.

The remaining figures illustrate various response pos-
sibilities for the intrinsic-conduction, loose-coupled sit-
uation with G/R effects negligible. Figure 4-a shows Z_T^*,
equivalent circuit, and $Y_T \equiv Z_T^{-1}$ results in the simplest
situation, that of bulk response only: $(r_p, r_n) = (\infty, \infty)$,
implying ohmic electrodes. Here, $C_1 = C_g \cong C^n$, $R_1 = R_B =$
R_∞, $\omega_B = \tau_D^{-1} = (R_\infty C_g)^{-1}$, and $G_\infty \equiv R_\infty^{-1} = {}^B(ez_e \mathcal{E}_i / \ell)(\mu_n + \mu_p)$.
Values of R_∞ (= R_D here) and C_g can only yield, in this
ordinary conduction case, estimates of ϵ and $(\mu_n + \mu_p)c_i$.

Somewhat more can be learned from the completely
blocking (0,0) case of Fig. 4-b. Here ω_B is as above but
ω' involves a mixture of bulk and interface parameters.
Define the Debye length for the present $z_n = z_p \equiv z_e$ case
as $L_D = [\epsilon kT/4\pi(ez_e)^2(n_e + p_e)]^{1/2}$ in the extrinsic-
intrinsic situation. The effective Debye length, L_e, is
in general a frequency-dependent function of χ, recombi-
nation,[7,8] and mobility parameters. For most practical
purposes, one may use $L_e = L_D$, however. In the intrinsic
case one should use $L_e \cong \sqrt{2}L_D$ for slow or zero $(c_i = N_i)$ re-
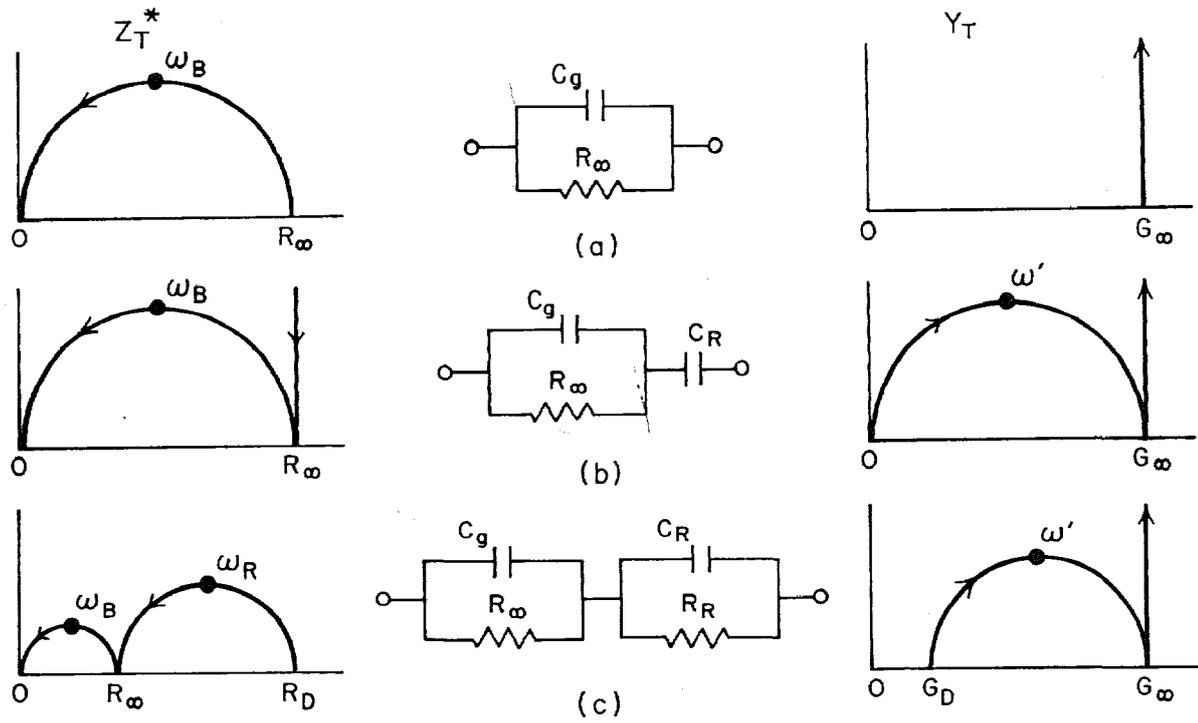combination under the following conditions: (a) $\mu_p = 0$, all

Figure 4. Response and equivalent circuits for (a) $(r_p, r_n) = (\infty, \infty)$; (b) (0,0); and (c) $(0, r_n)$, $\pi_m \gg 1$, and $r_n \gtrsim 1$.

Ω, and (b) $\mu_p \ll \mu_n$, $\Omega \stackrel{\sim}{>} \pi_m^{-1}$. In this latter case, the frequency is too high for positive charges to move appreciably in a half cycle and they thus act as if they were immobile. Let $M \equiv \ell/2L_D$ and $M_e \equiv \ell/2L_e$, always taken $\gg 1$ here. Then it is found[2,4] in the present case that $C_R \stackrel{\sim}{=} M_e C_g = \varepsilon/8\pi L_e$, just the double-layer capacitance of two layers (one at each electrode) in series. Here, where a value of C_R is available, ε, c_i, and $(\mu_n + \mu_p)$ can generally be found.

For the $(0, r_n)$ situation of Fig. 4-c, the material can be even better characterized. Here $C_{RN} \stackrel{\sim}{=} (M_e + r_n)$, $R_{RN} \stackrel{\sim}{=} 2/r_n$, and $\omega_R = \tau_R^{-1}$. One obtains the 4-b results when $r_n = 0$, of course. Here, where $\mu_n \gg \mu_p$, analysis yields estimates of ε, c_i, μ_n, and $k_n \equiv {}^n k_{no} \equiv {}^P k_{n\infty}$. This is the situation where an electrode reaction is the limiting chemical step. Note that $R_{DN} \equiv (1 + \pi_m^{-1})[1 + (2/r_n)] \stackrel{\sim}{=} 1 + R_{RN}$ in the present case.

Figure 5-a shows the complementary situation, that where diffusion is the limiting step. Note that here μ_n, the mobility of the discharging carrier, may be much smaller than that of the blocked carrier. The low-frequency arc of the Z_T^* diagram arises from the $k = 5$ term of Eq. (1). Its initial (high-frequency) slope is unity when $\alpha_5 = 0$, the only case considered here. The height of this arc is about $0.42 \, \pi_m^{-1} R_\infty$ and its width about $\pi_m^{-1} R_\infty$. Here $R_{DN} \stackrel{\sim}{=} 1 + \pi_m^{-1}$. Thus for $\pi_m \ll 1$, $\pi_m^{-1} R_\infty$, which is proportional to $[\mu_n (1 + \pi_m)]^{-1}$, involves essentially only μ_n, the smaller mobility. In the present case, τ_{5N} may be approximated by $bM^2[(2N_i - c_i)/c_i] \equiv [(2 + \pi_m + \pi_m^{-1})/4][(2N_i - c_i)/c_i]M^2$, which takes incomplete intrinsic dissociation $(c_i \stackrel{<}{\sim} N_i)$ into account. Thus, $\tau_5 \equiv \tau_{5N}\tau_D \stackrel{\sim}{=} (b\ell^2/2)(D_n + D_p)^{-1} \cdot [(2N_i - c_i)/c_i]$. Clearly, τ_5 can become very large and $\omega_W \stackrel{\sim}{=} 2.5\tau_5^{-1}$ very small when $c_i \ll N_i$. The present $k = 5$ term needs some modification[121] when $\pi_m \stackrel{<}{\sim} M^{-1}$. When $\pi_m \sim 1$, analysis of data of the present type can yield estimates of ε, c_i, μ_n, and μ_p if N_i is known independently or ε, N_i, μ_n, and μ_p if M (and thus c_i) is obtained independently. The reaction rate constant, ${}^1 k_n$, will be too large here $(r_n \gg 1)$ to be determinable from the data (reaction arc too small to measure).

The results of Fig. 5-b can appear when adsorption of a charged species on the electrode occurs.[5,6] The boundary parameter r_n is then complex, r_n^*, and may involve r_{no}, $r_{n\infty}$,
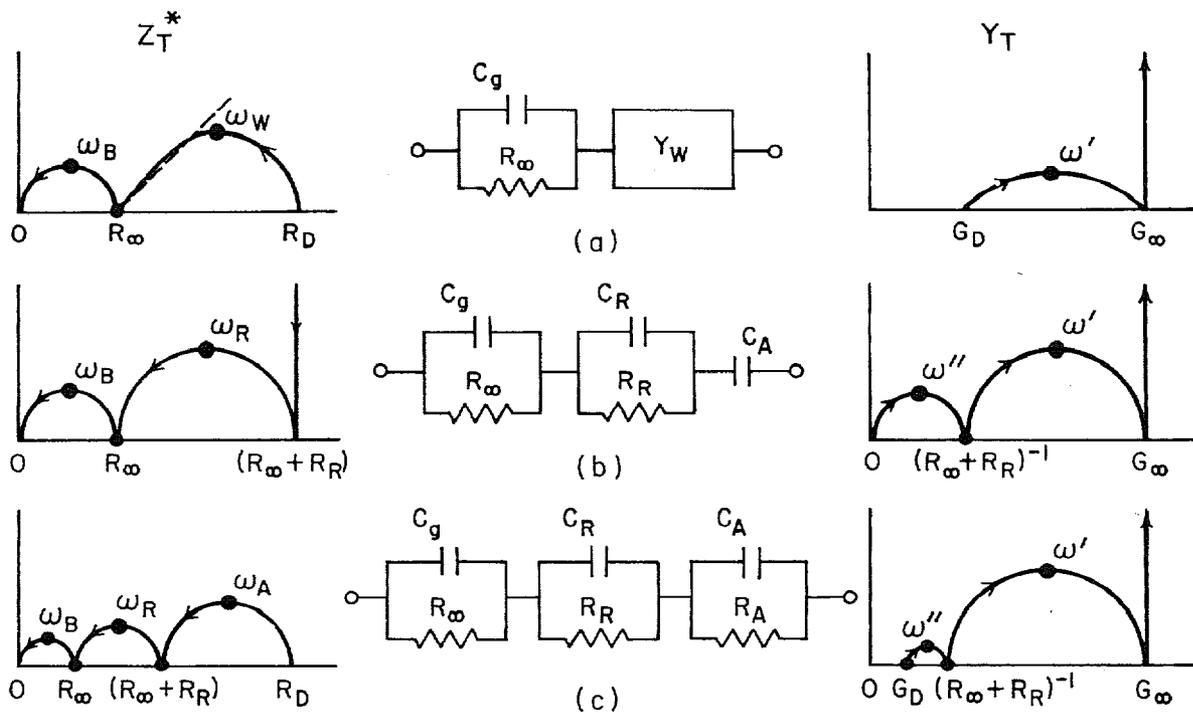
Fig. 5 Response and equivalent circuits for (a) $(0, r_n)$, $\pi_m \stackrel{\sim}{<} 1$, and $r_n \gg 1 + \pi_m^{-1}$; (b) $(0, r_n^*)$, $\pi_m \gg 1$, $r_{n\infty} \stackrel{\sim}{<} 1$, $r_{no} = 0$; and (c) like (b) but $r_{no} > 0$.
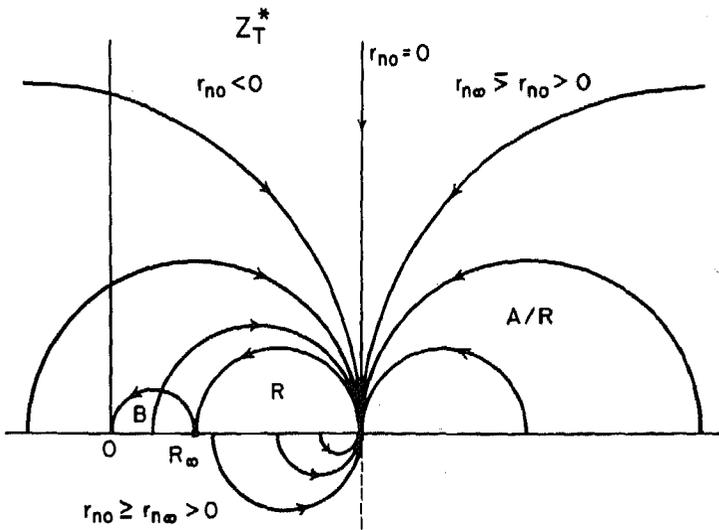
and $\xi_{An} \equiv \tau_{AN}/\tau_D$. In the loosely coupled case, $\xi_{An} \overset{\sim}{>}$ 100 M_e, and for $\pi_m \gg 1$, $C_{AN} \overset{\sim}{=} \xi_{An} r_{n\infty}/2$. Then, data analysis can yield estimates of ϵ, c_i, μ_n, $k_{n\infty}$, and τ_{AN}. The latter two quantities may themselves be expressed in terms of more basic properties of the system, as discussed elsewhere.[5] Note that when $R_R \gg R_\infty$ and frequency response measurements don't extend to high enough frequencies to delineate the bulk semicircle, the present adsorption-reaction results can be easily confused with the bulk-double layer response of Fig. 4-b. The two similar responses can be readily distinguished, however, on the basis of their extensive or intensive dependence. Further, note that 5-b shows that the electrode reaction semicircle may appear even in a kind of completely blocking situation, one where $R_D = \infty$. Unless frequency response measurements are extended to sufficiently low frequencies to show the beginning of the C_A capacitative rise, the presence of adsorption may not even be recognized.

The conditions appropriate for the results shown in Fig. 5-c are similar to those discussed above except that $r_{no} \neq 0$ and $r_{n\infty} \overset{\sim}{>} r_{no} > 0$. In this case, loosely coupled results are $C_{RN} \overset{\sim}{=} (M_e + r_{n\infty})$, $R_{RN} \overset{\sim}{=} (2/r_{n\infty})$, $C_{AN} \overset{\sim}{=} \xi_{An} r_{n\infty}^2/2r_{nm}$, and $R_{AN} \overset{\sim}{=} 2\overset{\overbrace{}}{r}/r_{n\infty} r_{no}$, where $r_{nm} \overset{\sim}{=} r_{n\infty} \overset{\sim}{=} r_{no}$. Here, $R_{DN} \overset{\sim}{=} (1 + \pi_m^{-1})[1 + (2/r_{no})] \equiv 1 + R_{RN}^{nm} + R_{AN} \overset{\sim}{=} 1 + (2/r_{no})$. The radial frequency at the peak of the A/R arc, ω_A, becomes, in the present case, $\omega_A = (\tau_D R_{AN} C_{AN})^{-1} \overset{\sim}{=} \tau_{AN}^{-1}(r_{no}/r_{n\infty})$. It turns out for the situation of Fig. 5-c that as coupling increases and ξ_{AN} decreases below $\sim$ 100M_e, $\omega_3 \equiv \tau_3^{-1}$ always remains larger than ω_2. In fact, C_{3N} decreases from the above $C_{AN} \gg C_{RN}$ value and approaches the smaller uncoupled C_{RN} value of M_e, while C_{2N} simultaneously increases above this value. At the same time, R_{2N} decreases toward zero and R_{3N} increases toward $R_{DN} - 1 \overset{\sim}{=} (2/r_{no})$. Thus, for sufficiently small ξ_{AN}, $Z_{2N} \to 0$, and Z_{3N} then plays the reaction role, involving as before the double-layer capacitance and a reaction resistance of $(2/r_{no})R_\infty$ instead of the uncoupled R_R value of $(2/r_{n\infty})R_\infty$. The original reaction arc disappears and its place is filled by what was, in the loosely coupled region, the adsorption-reaction arc. Therefore, if only a single reaction arc is present, it will usually be impossible to establish which of $r_{n\infty}$ or r_{no} is involved, although they are of course identical in the absence of adsorption.
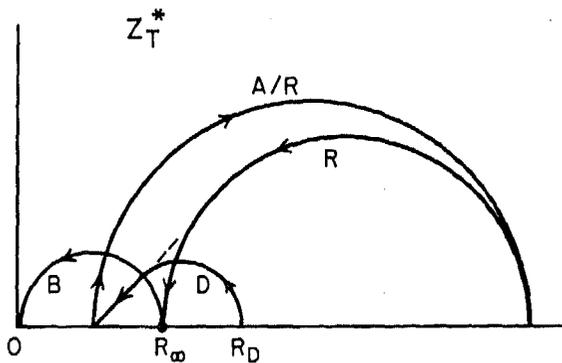
There are numerous further curve-shapes which can arise from $Z_3 \cong Z_A$ in the loosely-coupled situation. Some of them appear in Fig. 6-a. Note that when $r_{no} > r_{n\infty}$, $r_{nm} < 0$ and both C_{AN} and R_{AN} are negative, leading to the negative-capacitance arcs shown below the real axis. The largest such semicircle, appearing for $r_{no} \to \infty$, is the mirror image of the reaction semicircle. Further when $-2 < r_{no} < 0$, $R_{DN} < 0$, and thus the differential resistance of the system is negative in the low frequency limit. The result of Fig. 6-b shows that a diffusion arc may appear at even lower frequencies than the reaction and A/R arcs. Experimental results of just this form have been found by Gabrielli.[16]

Finally, Fig. 7 shows some further possible combinations of R, A/R, and D arcs. Typical parameter values yielding results similar to those of Fig. 7-a and 7-b are $r_{n\infty} = 10^9$, $r_{no} = 0$ for 7-a and 2 for 7-b, $\xi_{An} = 2$, $\pi_m = 10^{-1}$, and $M = M_e = 10^3$. Values leading to shapes similar to 7-c and 7-d are $r_{n\infty} = 6$, $r_{no} = 0$ for 7-c and 2 for 7-d, $\xi_{An} = 4 \times 10^8$, $\pi_m = 10^{-1}$, and $M = M_e = 10^3$. Notice that the large decrease in $r_{n\infty}$ has been compensated by a large increase in ξ_{An} so that C_{AN} is roughly the same in the a, b and c, d cases. Many other arc combinations are possible. For example, any of the A/R arc shapes of Fig. 6-a could occur at the right of the 7-c and 7-d diagrams, not just those shown.

In conclusion, it is worthwhile to summarize some general expressions which should be useful for data analysis in arbitrary $(0, r^*)$, π_m, and conduction-type situations. Let[1] $\pi_f \equiv n^*/p^* \cong (\phi + \chi)/(\phi - \chi)$, where $\phi \equiv (1 + \chi^2)^{1/2}$. Here $\chi \gg 1$ for strong n-type doping; $\chi = 0$ for intrinsic conditions; and $\chi \ll -1$ for strong p-type doping. Further, define $\delta_n \equiv \pi_f/(1 + \pi_f)$ and $\varepsilon_n \equiv \pi_e/(1 + \pi_e)$, where $\pi_e \equiv \pi_m \pi_f$. Then $R_{DN} = \varepsilon_n^{-1}[1 + (2/r_{no})]$. For loose coupling one finds: $R_{1N} \cong R_{BN} \cong 1$, $C_{1N} \cong C_{BN} \cong 1$; $R_{2N} \cong R_{RN} \cong 2/\varepsilon_n r_{n\infty}$, $C_{2N} \cong C_{RN} \cong M_e + \varepsilon_n r_{n\infty}$; and $R_{3N} \cong R_{AN} \cong 2r_{nm}/\varepsilon_n r_{n\infty} r_{no}$, $C_{3N} \cong C_{AN} \cong \xi_{An}(\varepsilon_n r_{n\infty})^2/2\varepsilon_n r_{nm}$. As already mentioned, Z_{4N} will often be negligible compared with the other contributions to Z_{TN}. The π_m appearing in the fifth term of Eq. (1) should be replaced by the more general π_e. The approximate expression for τ_{5N} already given above may be used (with the factor b given more generally[1]) in the Z_{5N} part of Eq. (1)

Z_T^*

$r_{no} < 0$ $r_{no} = 0$ $r_{n\infty} \gtrless r_{no} > 0$

A/R

R

B

O R_∞

$r_{no} \gtrless r_{n\infty} > 0$

(a)

Z_T^*

A/R

R

B   D

O R_∞ R_D

(b)

Fig. 6   Further $(0, r_n^*)$ response for (a) $\pi_m \gg 1$, $r_{n\infty} \stackrel{\sim}{<} 1$, and various values of r_{no}. (b) As in (a) but $\pi_m \stackrel{\sim}{<} 1$ and $-\infty < r_{no} < -2$.
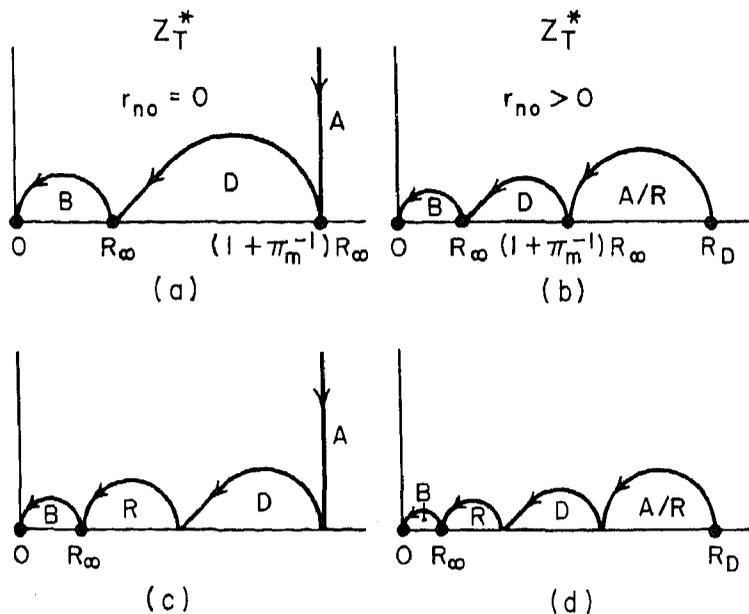
Fig. 7 Additional $(0, r_n^*)$ response possibilities.

or its $\alpha_5 \neq 0$ generalization. The quantity M_e usually may be taken as M multiplied by a factor dependent on π_m, recombination, and δ_n. This factor reduces to $\delta_n^{1/2}$ in the $\pi_m \gg 1$, $\approx$ full dissociation situation.

REFERENCES

1. J. R. Macdonald, J. Chem. Phys. $\underline{58}$, 4982 (1973).
2. J. R. Macdonald in Electrode Processes in Solid State Ionics, edited by M. Kleitz and J. Dupuy (D. Reidel Publishing Co., Dordrecht-Holland, 1976).
3. J. R. Macdonald, J. Electroanal. Chem. $\underline{53}$, 1 (1974).
4. J. R. Macdonald, J. Chem. Phys. $\underline{61}$, 3977 (1974).
5. J. R. Macdonald, J. Electroanal. Chem. $\underline{70}$, 17 (1976).
6. J. R. Macdonald and P.W.M. Jacobs, J. Phys. Chem. Solids, to be published.
7. J. R. Macdonald, J. Chem. Phys. $\underline{29}$, 1346 (1958).
8. J. R. Macdonald, J. Phys. C: Solid State Phys. $\underline{7}$, L327 (1974); $\underline{8}$, L63 (1975).

9. A. R. von Hippel, Dielectrics and Waves, (John Wiley, New York, 1954), pp. 228-234.
10. J. Volger, Prog. in Semiconductors 4, 207 (1960).
11. R. B. Hilborn, Jr., J. Appl. Phys. 36, 1553 (1965).
12. G. S. Nadkarni and J. G. Simmons, J. Appl. Phys. 47, 114 (1976).
13. K. S. Cole and R. H. Cole, J. Chem. Phys. 9, 341 (1941).
14. J. R. Sandifer and R. P. Buck, J. Electroanal. Chem. 56, 385 (1974).
15. D. W. Davidson and R. H. Cole, J. Chem. Phys. 23, 493 (1955).
16. G. Gabrielli, Ph.D. thesis, University of Paris, 1973; Métaux, Corrosion, Industrie Nos. 573, 574, 577, 578 (1973).